Dependence of Extreme Daily Maximum Temperatures on Antecedent Soil Moisture in the Contiguous United States during Summer

IMKE DURRE AND JOHN M. WALLACE

Department of Atmospheric Sciences, University of Washington, Seattle, Washington

DENNIS P. LETTENMAIER

Department of Civil Engineering, University of Washington, Seattle, Washington

(Manuscript received 8 October 1998, in final form 13 October 1999)

ABSTRACT

The paper presents an analysis of the dependence of summertime daily maximum temperature on antecedent soil moisture using daily surface observations from a selection of stations in the contiguous United States and daily time series of soil moisture computed with a simple local water balance model. The computed soil moisture time series are offered as an alternative to Palmer's soil moisture anomaly (Z) index, the Palmer Drought Severity Index (PDSI), and other such time series. In contrast to other water balance models that have been designed for the computation of soil moisture time series, the model herein is driven by daily rather than monthly data, uses the Priestley–Taylor method in lieu of Thornthwaite's method to calculate potential evapotranspiration, allows for runoff during dry periods as well as when soil moisture is not at field capacity, includes a crude scheme for taking into account the effects of snowmelt on the water balance, and permits geographical variations in soil water capacity. The Priestley–Taylor method is considered to yield more realistic estimates of evapotranspiration than Thornthwaite's method since it accounts for net radiation and represents a special case of the widely used Penman–Monteith method. Total runoff is parameterized according to the Variable Infiltration Capacity model. Based on a comparison with soil moisture measurements at Peoria, Illinois, the model appears to simulate the variability of soil moisture anomalies (W') reasonably well.

Analysis of the relationship between W' and daily maximum temperatures (T_{max}) shows that in the central and eastern United States during the summer, the entire frequency distribution of standardized T_{max} is shifted toward higher values following a ''low-W''' day (i.e., a day on which W' falls into the bottom quartile of its frequency distribution). The shift is most pronounced at the high end of the temperature distribution, indicating that as the soil gets drier, hot days tend to get hotter to a greater degree than cool days get warmer. Over the southeastern United States, where local evapotranspiration contributes a significant portion of the moisture available for precipitation, the temperature signal is particularly prominent and persists for up to several weeks after the soil moisture anomaly is observed. The relationship between temperature and daily precipitation is found to be much weaker and less persistent than the T_{max}–W' association. Thus, the frequency of record and near-record high temperatures is shown to be sensitive to soil moisture conditions, particularly on timescales shorter than one month.

1. Introduction

The summers of 1934, 1936, 1952–54, 1980, and 1988 were characterized by above-normal temperatures, below-normal precipitation, and a deficit in soil moisture over large areas of the central and eastern United States (Diaz 1983; McNab 1989), and many more summers have been marked by more regional drought/heat wave episodes. The tendency for above-normal summertime temperatures to coincide with periods of below-normal precipitation has been illustrated in many empirical studies. During summer, strong negative monthly and seasonal contemporaneous correlations between mean temperature and total precipitation are observed over the Southern Great Plains of the United States, and weaker correlations in the same sense are found along the eastern seaboard as well as in California, the Pacific Northwest, and the Great Lakes region (Crutcher 1978; Madden and Williams 1978; Namias 1983; Williams 1992; Huang and van den Dool 1993; Zhao and Khalil 1993). Tables of regional temperature rankings for the driest 10% of the summers on record reflect similar geographical variations in the strength of the inverse temperature–precipitation relationship (Karl and Quayle 1981; McNab 1989). While dry summers in New England, the mid-Atlantic region, and states along the Pacific coast are about equally likely to have above-median

Corresponding author address: Imke Durre, JISAO, Box 354235, University of Washington, Seattle, WA 98195.
E-mail: imke@atmos.washington.edu

or below-median temperatures, the driest summers in the Southeast are consistently among the warmest on record.

Huang and van den Dool (1993) have shown that the correlation between precipitation and temperature is significantly larger when precipitation leads temperature by one month than when temperature leads precipitation. Furthermore, both Walsh et al. (1985) and Huang and van den Dool (1993) found that the inclusion of monthly mean precipitation in addition to monthly mean temperature improves the prediction of subsequent monthly mean temperature in the interior central and southeastern United States, particularly during the warm season. Over northern Texas, Oklahoma, and Kansas, precipitation alone turned out to be the best predictor in Huang and van den Dool's analysis. These findings support the widely held notion that, at least during summer, there exists a memory of past precipitation in the interior of continents.

It has been widely speculated that this memory is provided by the land surface through a positive feedback between soil moisture anomalies and atmospheric anomalies that act to maintain hot, dry conditions (e.g., Namias 1960; Rind 1982; Shukla and Mintz 1982). According to this hypothesis, a depletion in the amount of water in the soil that is brought about by a deficit in precipitation causes the rate of surface evapotranspiration to decrease. The reduced evapotranspiration is associated with a repartitioning of the surface heat fluxes in favor of the sensible heat flux, which requires a warmer surface and planetary boundary layer. The higher temperatures, in turn, tend to enhance the drying of the soil and lower atmosphere. This feedback is expected to operate particularly during summer, when the surface latent heat flux tends to be large. Additional feedbacks may involve changes in cloudiness, relative humidity, heat capacity, surface albedo, and surface roughness (Bravar and Kavvas 1991; Huang and van den Dool 1993).

Evidence in support of the existence of a land–atmosphere feedback comes from numerical experiments as well as from analyses of the relationships between computed indices of soil moisture and observed meteorological conditions. General circulation model simulations of the summer climate in which the initial distribution of soil moisture is varied indicate that a dry soil is associated with low evaporation rates and a warm, dry boundary layer, while a wet soil tends to have the opposite effect (Rind 1982; Shukla and Mintz 1982; Yeh et al. 1984; Yang et al. 1994). Furthermore, the correlations between monthly precipitation and the next month's mean temperature based on multiyear runs of the National Centers for Environmental Prediction's Medium-Range Forecast Model resemble the observed correlation pattern over the United States only when the soil moisture in the model is allowed to interact with the atmosphere (Huang and van den Dool 1993).

For lack of a network of soil moisture observations, empirical studies of soil moisture–temperature relationships over the United States have generally employed estimates of soil moisture based on meteorological observations. Walsh et al. (1985), for example, calculated a soil moisture depth parameter whose time rate of change equals the difference between actual precipitation and computed evapotranspiration. More sophisticated water balance models that include the effects of runoff have been used for the computation of the widely used Palmer *Z* and Drought Severity Indices (PDSI; Palmer 1965), as well as in a study by Huang et al. (1996) that explored the possibility of generating a monthly soil moisture dataset for the United States. Georgakakos et al. (1995), on the other hand, applied a full-fledged hydrological model with a daily, rather than monthly, time step to two watersheds in the U.S. Great Plains in order to study land–atmosphere interaction. All of these methods produce soil moisture proxies that appear to be reasonably consistent with observations of precipitation, runoff, and soil moisture where available.

Studies based on the various soil moisture indices have generally yielded similar soil moisture–temperature relationships. Regardless of the analysis method or soil moisture parameter used, the results for warm-season months indicate that, particularly for inland, nonarid areas, a wet soil tends to depress the concurrent and subsequent monthly mean temperature, while a drier-than-normal soil is favorable for higher-than-expected monthly mean temperatures (Walsh et al. 1985; Karl 1986; Chang and Wallace 1987; Williams 1992). Furthermore, contemporaneous soil moisture–temperature correlations are consistently more negative than correlations between precipitation and temperature (Huang et al. 1996). When predicting monthly mean temperatures, the inclusion of antecedent soil moisture in addition to antecedent temperature can enhance the predictive skill over large portions of the interior United States during the warm season, particularly at lags of several months (Huang et al. 1996). According to Karl (1986), the relatively weak dependence of temperature on antecedent soil moisture anomalies in arid regions such as the Southwest stems from the fact that the magnitude of surface evapotranspiration is low in these areas, even during periods of above-normal precipitation. Due to processes such as stratus clouds, sea breezes, and general onshore advection, which can suppress daytime temperatures (Walsh et al. 1985; Karl 1986), soil moisture tends to also be only weakly associated with subsequent temperature along the Pacific and Atlantic coasts.

Since evapotranspiration takes place primarily during the day, it follows that daytime temperatures should be more sensitive to variations in soil moisture than nighttime temperatures. This hypothesis is supported by the findings of Chang and Wallace (1987), Williams (1992), Georgakakos et al. (1995), and Huang et al. (1996). Using 5-day mean soil moisture time series computed

for the Bird Creek, Oklahoma, and Boone River, Iowa, watersheds with a rainfall–runoff–routing model, Georgakakos et al. (1995) showed that, at Bird Creek during the summer, the correlation between soil moisture and daily maximum temperature peaks when soil moisture leads maximum temperature by 5–10 days. At Boone River, on the other hand, the highest correlation is found at zero lag. Based on these results it appears that the strength of the local land–atmosphere feedback varies geographically even on the timescale of days. Furthermore, temperature appears to be more sensitive to negative soil moisture anomalies than to positive ones (Georgakakos et al. 1995), indicating that the relationship between soil moisture and temperature may be nonlinear. Williams (1992) noted that the highest recorded temperature in July tends to be higher during dry spells than during wet spells, suggesting that at least the top half of the distribution of maximum temperatures is shifted towards higher values under dry conditions.

In this study, we seek to extend the work of Williams (1992), Georgakakos et al. (1995), and Huang et al. (1996). A simple water balance model similar to the one described by Huang et al. is used to compute soil moisture time series from observed precipitation and temperature. As in Huang et al., the use of a simple water balance model in lieu of a more complex rainfall–runoff–routing model such as that employed by Georgakakos et al. is the vehicle for extending the analysis of data from two watersheds to locations across the United States. However, in order to be able to examine local soil moisture–temperature relationships on daily timescales as in Georgakakos et al., the model is driven by daily station observations rather than by monthly climate division data. Other changes to Huang et al.'s approach include the estimation of potential evapotranspiration by the Priestley–Taylor method (Priestley and Taylor 1972) rather than by Thornthwaite's method, the incorporation of geographically varying soil water capacity as well as a crude treatment of snow, and the implementation of the Variable Infiltration Capacity (VIC) parameterization (Stamm et al. 1994) for the computation of runoff. The time series of daily soil moisture generated by this model are then used to compare the distribution of summertime daily maximum temperatures at 80 stations across the contiguous United States under conditions of anomalously dry and anomalously wet soil. This approach permits the examination of the sensitivity of extreme daytime temperatures to soil moisture variations.

The remainder of the paper is organized as follows. After a description of the data in the next section, section 3 describes the design and verification of the water balance model employed in this study. Analyses of temperature–soil moisture relationships are presented in section 4 and a discussion of the results follows in section 5.

2. Data

The data used in this study include daily surface observations at selected stations across the contiguous United States, estimated total available water capacities near the stations, observed soil moisture at Peoria, Illinois, and monthly values of the PDSI and soil moisture anomaly (Z) index for the climate divisions in which the chosen stations are located. The period of record examined is January 1948–December 1995.

Daily maximum and minimum temperatures (in whole degrees Fahrenheit), precipitation (in hundredths of inches), and percent of possible sunshine for a set of 80 U.S. stations were taken from the First Order Summary of the Day dataset [National Climatic Data Center 1998a]. The selection of sites was made on the basis of geographical location and data availability. A map of the station locations is shown in Fig. 1. These data are used as input time series to the soil moisture model as well as for subsequent analyses.

The water balance model described in the next section requires the specification of the maximum soil water content ($W_{\max}$). For each station analyzed, this parameter was derived from the International Soil Reference Information Centre's World Inventory of Soil Emissions Potentials Database (ISRIC-WISE) Soil Moisture Retention dataset that provides estimated ranges of total available water capacity in the top 0–1 m of soil on a global 0.5×0.5 latitude–longitude grid (Batjes 1996). In the dataset, water capacities are expressed as equivalent depths and listed as ranges (e.g., 90–150 mm or $\geq$ 200 mm). In most cases, $W_{\max}$ for a particular station was taken to be equal to the value at the center of the water capacity range given for the land grid point nearest the station. For the ranges $\leq$90, $\geq$150, and 200–500 mm, values of 75, 150, and 200 mm were chosen since they appeared to best fit into the geographical distribution of water capacities. Although $W_{\max}$ lies between 105 and 135 mm at most stations, it ranges as low as 75 mm and as high as 200 mm. Numerical experiments with the model indicate that the results of this study are not very sensitive to the choice of maximum soil water content.

Biweekly to monthly soil moisture observations at Peoria, Illinois, as well as the PDSI and Z index are used to verify the results of this study. The soil moisture observations were taken in 11 layers between the surface and a depth of 2 m with a neutron probe on a biweekly to monthly basis as part of the Illinois Climatology Network. A detailed discussion of the measurements can be found in Hollinger and Isard (1994). The PDSI and Z indices are part of the Time-Bias Corrected Temperature–Precipitation–Drought Index dataset [National Climatic Data Center 1998b]. They are derived from monthly mean temperature and precipitation in a multistep process that begins with the application of a simple bucket model in an effort to estimate the moisture deficit of a region. For further information, the reader

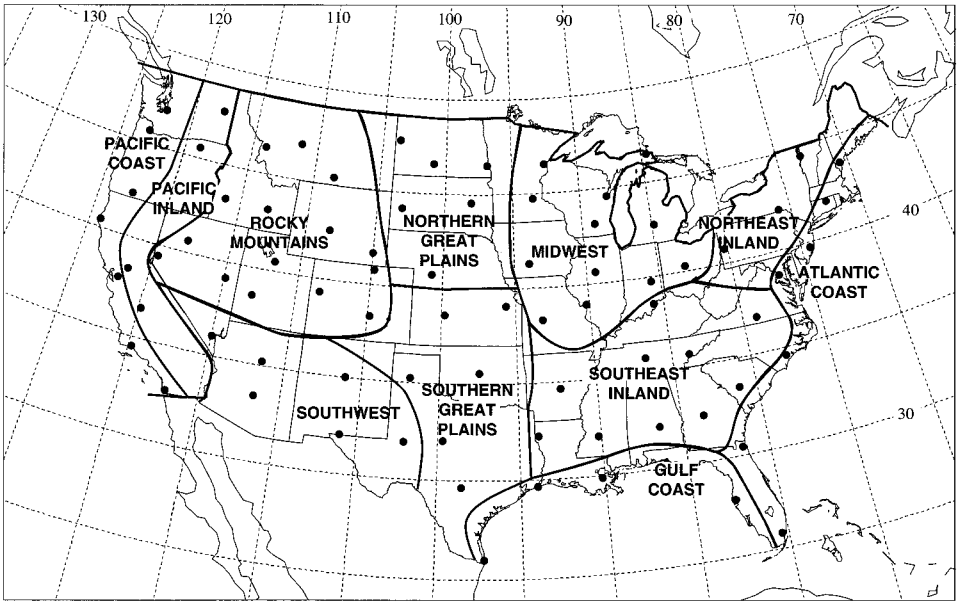

FIG. 1. Map of stations (dots) and geographical regions included in this study.

is referred to the dataset documentation and Palmer's (1965) report on the procedure for computing these indices.

3. Model description and verification

A daily time series of soil moisture is derived for each station by means of a simple local water balance model with a daily time step. The model is driven by daily temperature and precipitation observed at the station. Locally, the time rate of change in the amount of water (W) in the top layer of the soil is assumed to depend on the amount added by precipitation (P) minus the losses resulting from evapotranspiration (E) and total runoff (R). Thus, the basic equation of the model is

$$\frac{dW}{dt} = P - E - R. \tag{1}$$

As will be described later in this section, precipitation is assumed to consist of rainfall (P_r) and snow melt (M):

$$P = P_r + M. \tag{2}$$

In the absence of snow on the ground, evapotranspiration is computed from potential evapotranspiration (E_p) and an evaporation efficiency factor (β):

$$E = \beta E_p. \tag{3}$$

Following the work of Manabe et al. (1965), evapotranspiration is assumed to occur at the potential rate when the soil is more than 75% saturated and to decrease linearly with soil moisture below this threshold. Thus, β is expressed as

$$\beta = W/W_{\max} \quad \text{for } W/W_{\max} < 0.75 \quad \text{and} \tag{4a}$$

$$\beta = 1 \quad \text{for } W/W_{\max} \geq 0.75, \tag{4b}$$

where $W_{\max}$ is the maximum soil moisture content. The value of $W_{\max}$ for each station is derived from the ISRIC–WISE Soil Moisture Retention dataset as described in the previous section.

Potential evapotranspiration E_p is calculated according to the Priestley–Taylor method (Priestley and Taylor 1972), setting the Priestley–Taylor parameter α equal to 1.26 and the ground heat flux equal to 10% of the net solar radiation at the surface (Kimball et al. 1997). Daily net solar radiation at the surface is expressed as a function of latitude, elevation, day of the year, surface albedo, and diurnal temperature range ($T_{\max} - T_{\min}$), following Buffo et al. (1972), Swift (1976), and Bristow and Campbell (1984). In this formula, the diurnal temperature range serves as an indicator of the amount of radiation that is attenuated by the atmosphere and the albedo of the ground is fixed at 0.2.

Runoff is computed using a VIC parameterization (Stamm et al. 1994) that allows for soil moisture drainage during dry periods and subgrid-scale spatial variability in soil moisture capacity. Total runoff is divided into two components, base flow (Q_b) and direct runoff (Q_d):

$$R = Q_b + Q_d. \tag{5}$$

Base flow is assumed to be proportional to soil moisture storage:

$$Q_b = k_b W. \tag{6}$$

Following Stamm et al., the base flow parameter k_b is

fixed at 0.005 day^{-1}. This component of the total runoff ensures that some soil moisture drainage occurs regardless of the amount or type of precipitation.

Direct runoff due to rainfall and snowmelt is parameterized as follows (Stamm et al. 1994). Letting I_0 the initial infiltration capacity of a grid cell, W_0 equal the initial soil moisture content, and I_{max} the maximum infiltration capacity within the grid cell, the form of the area-averaged direct runoff depends upon whether or not the sum of I_0 and any rainfall or snowmelt on the current day exceeds I_{max}:

$$Q_d = P - W_{max} + W_0 \quad \text{for } I_0 + P \geq I_{max} \quad \text{and} \tag{7a}$$

$$Q_d = P - W_{max} + W_0 + W_{max}\left[1 - \left(\frac{(I_0 + P)}{I_{max}}\right)^{1+B}\right] \quad \text{for } I_0 + P < I_{max}. \tag{7b}$$

Here, B is a shape, or infiltration parameter that is fixed at 0.3, I_{max} is related to W_{max} by the formula

$$I_{max} = \frac{W_{max}}{1 + B}, \tag{8}$$

and I_0 is defined as

$$I_0 = I_{max}[1 - (1 - A)^{1/B}]. \tag{9}$$

The fractional area A of the grid cell with infiltration capacity less than I_0 is given by

$$A = 1 - \left[1 - \left(\frac{W_0}{W_{max}}\right)^{\frac{B}{1+B}}\right]. \tag{10}$$

Thus, in the presence of precipitation, direct runoff occurs not only when the soil is saturated but also under certain conditions when the soil water content is not at its maximum capacity. By definition, Q_d is set to zero when both rainfall and snowmelt are equal to zero.

Whenever there is no snow on the ground, the soil moisture is first adjusted for evapotranspiration and base flow, which are based on the previous day's soil moisture. Direct runoff is then calculated from the adjusted soil moisture and the current day's rainfall and snowmelt. Finally, the current day's soil moisture is obtained by adding the rainfall and snowmelt to the adjusted soil moisture and subtracting the direct runoff (Stamm et al. 1994). Any precipitation that falls when the day's mean temperature (i.e., the average of day's maximum and minimum temperatures) is below freezing is considered to fall as snow. When snow is on the ground, two separate water budgets are maintained for the soil and the snow. Both evapotranspiration from the soil and direct runoff are set to zero, while base flow is allowed to continue in accordance with Eq. (6). In addition, snow is assumed to sublimate at an estimated potential rate that is derived from the Priestley–Taylor formula by substituting the latent heat of sublimation for the latent heat of vaporization and changing the surface albedo from 0.2 to 0.8. While the daily mean temperature remains below freezing, the water equivalent of the snow on the ground changes as a result of sublimation and any new snowfall. As soon as the daily mean temperature rises above 0°C, all of the snow is melted, the water equivalent of the melted snow is added to the day's precipitation, and evapotranspiration and direct runoff are allowed to resume. Although this treatment of snow is very crude, it appears to be sufficient for a reasonable simulation of soil moisture during the warm season. Experiments with albedos of 0.15 for bare ground and 0.7 for a snow-covered surface indicate that although soil moisture values are slightly lower when the surface albedo is decreased, soil moisture variability and therefore the results of this study are unaffected.

In summary, the model requires latitude, altitude, maximum soil water content, surface albedo, as well as time series of daily maximum and minimum temperature and precipitation as input and supplies daily time series of evapotranspiration, base flow, direct runoff, and soil moisture as output. The parameters include the Priestley–Taylor parameter, the evaporation efficiency factor, the base flow coefficient, and the shape parameter. Using the model, time series of daily soil moisture were calculated for each of the stations shown in Fig. 1. Since the previous day's soil moisture as well as the current day's temperature and precipitation are essential to the computation of each soil moisture value, the length of the resulting time series at a particular station depends on the length of the continuous record of precipitation and temperature. At most stations, the time series extend over a period of more than 30 yr and all stations have a continuous record of at least 20 yr.

To verify that the daily soil moisture time series generated by the model are realistic, the time series computed for Peoria, Illinois, was compared to soil moisture measurements taken at that site during the common period of record of 1983–88 (Hollinger and Isard 1994). Experiments with several values of W_{max} and soil moisture observations to various depths indicate that at Peoria, the best agreement between computed and measured soil water content is achieved when W_{max} in the model is set to 120 mm, as suggested by the ISRIC–WISE dataset, and observations for the top 0.3 m of soil are considered. Using monthly input data and a different water balance model, Huang et al. (1996) found the correlation between observed and simulated soil moisture to be largest for the top 1.3 m of the soil. This discrepancy between our and Huang et al.'s results is consistent with the fact that the timescale of soil moisture variations has been shown to increase with increasing depth (Isard and Hollinger 1994; Georgakakos et al. 1995). The observed and computed time series for Peoria that exhibit the highest correlation with each other are shown in Fig. 2a. To facilitate the comparison, computed values (black dots) are plotted only on those dates for which measurements (gray vertical lines) are available. Over the entire 6-yr period (116 samples), the correlation coefficient between the two time series is

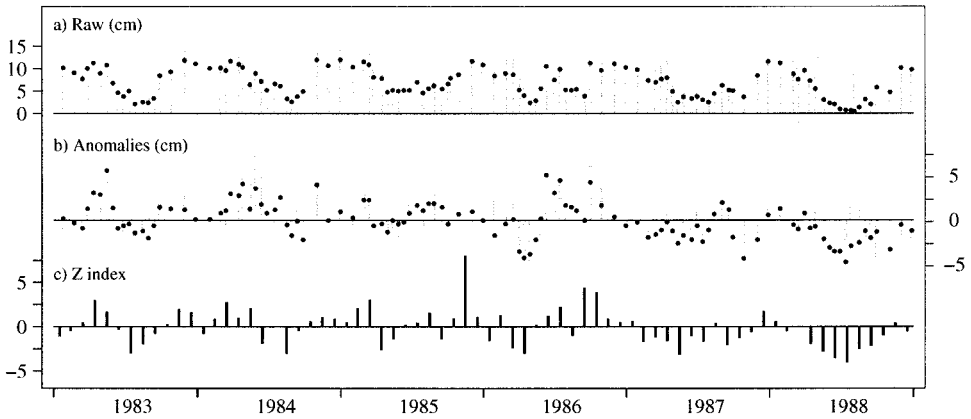

FIG. 2. Time series for 1983–88 of (a) raw observed and computed soil moisture content (cm) at Peoria, Illinois; (b) observed and computed soil moisture anomalies (cm) at Peoria; and (c) the Palmer *Z* index for the climate division of Peoria. In (a) and (b), observations are given for the top 30 cm of the soil and are plotted as gray vertical lines. Measurements were taken approximately once a month between Oct and Feb and once every two weeks between Mar and Sep; three observations are missing. Computed values are identified by black dots and are plotted only on days on which observations are available.

0.86. However, *W* deviates significantly from the observations in late winter and early spring when snowmelt strongly affects soil moisture. During summer, the computed values, on average, are not quite as low as the measurements. Nevertheless, the soil moisture anomalies for May–September of 1983–88 (48 samples) are correlated at a level of 0.73.

Figure 2b displays standardized time series of the observed and computed soil moisture at Peoria, while Fig. 2c shows the end-of-the-month *Z* index for the climate division in which Peoria is located. With the annual cycle removed, the correlation between *W* and observed soil moisture drops to 0.77. The *Z* index, on the other hand, is correlated with the soil moisture observations at a level of only 0.53. Two factors are likely to be primarily responsible for the difference in the correlations for *Z* and *W*. First, *Z* represents an area average over a climate division, whereas *W* exhibits variability at one station. Second, the use of monthly rather than daily data in the computation of the *Z* index is likely to introduce errors in the estimation of runoff and evapotranspiration (Alley 1984). The level of agreement between the soil moisture measurements and *W* at Peoria suggests that for the purpose of studying local climatic relationships during the warm season, the model-calculated soil moisture can be used as a reasonable proxy for the observations.

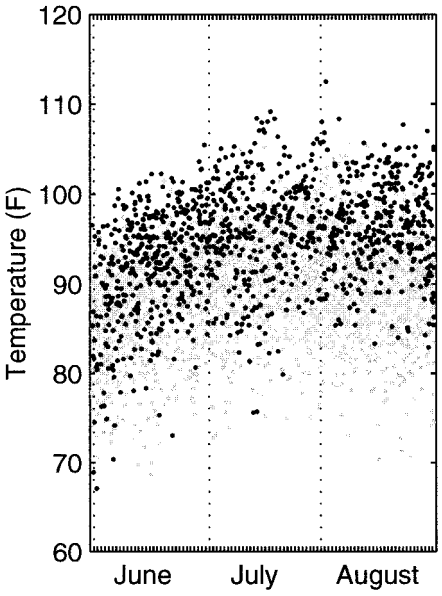

FIG. 3. Distribution of Jun–Aug (JJA) daily maximum temperatures for 1949–95 at Little Rock, Arkansas. Calendar days are plotted along the *x* axis, temperatures (in °F) along the *y* axis. Temperatures observed on the day after a soil moisture anomaly (W') that falls into the lowest quartile of all of the station's JJA W' values are shown in black.

4. Local soil moisture–temperature relationships

In order to examine the sensitivity of daytime temperatures to low-soil moisture conditions, the summertime (June–August) values of W' at each station are stratified into ''low'' and ''other'' values. A day's value of W' is defined as low if it lies in the bottom quartile of the station's summertime W' distribution. Figure 3 displays the distribution of T_{max} for June–August at Little Rock, Arkansas. Here, each black dot represents a temperature that is observed on a day following a low-W' day. Since temperatures in the dataset are reported in whole degrees Fahrenheit, this unit of measurement has been retained in the plot. (To prevent the dots from clustering at integer values of temperature and time, the data points have been dispersed into 1°F $\times$ 1 day rectangles by adding to each temperature and time a number drawn from a uniform random distribution with a half-width of 0.5.)

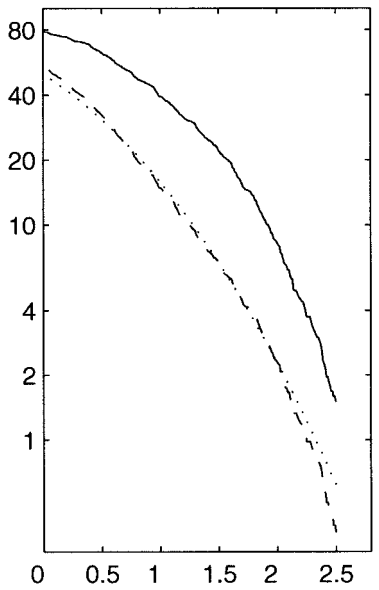

FIG. 4. Cumulative probability distribution functions of standardized daily maximum temperatures (T^*_{max}) based on summer low-W' days (solid line), all summer days (dashed line), and the assumption that T^*_{max} follows a normal distribution (dotted line). The T^*_{max} thresholds are plotted on the abscissa, the percentage of T^*_{max} greater than a given threshold on the ordinate, on a logarithmic scale.

An alternative method of presenting this information is to plot the cumulative probability distribution function (PDF) of standardized daily maximum temperatures (T^*_{max}) at Little Rock for all summer days as well as for low-W' days (Fig. 4). For this purpose, each T_{max} is standardized using the annual cycles of the means and standard deviations of T^*_{max} as approximated by the first four harmonics of their respective raw climatologies. To derive the low-W' PDF, the percentage of summer low-W' days that are immediately followed by a day with T^*_{max} greater than a certain threshold is calculated for a range of thresholds. For the all-day PDF, summer days with any W' value are included. To emphasize the difference between the tails of the distributions, the natural logarithm of each PDF has been plotted.

Figures 3 and 4 show that at Little Rock, hot summer days are more likely during times of low soil moisture than at other times. Of the 1174 observations of $T_{max} \geq 95$°F, 605 (52%) occurred on a day immediately following a low-W' day. Considering that, by definition, low-W' days account for only 25% of all days, the incidence of such days is about twice as high as would be expected by chance. The fraction of temperatures observed on the day following a low-W' day is even larger for more extreme temperatures: 220 of the 285 days with $T_{max} \geq 100$°F and 34 of the 38 days with $T_{max} \geq 105$°F occurred under low-W' conditions. In agreement with previous studies (Williams 1992; Georgakakos et al. 1995; Huang et al. 1996), the association between daily minimum temperature and soil moisture anomalies at Little Rock (not shown) is much less pronounced than the T_{max}–W' relationship.

TABLE 1. Regional values of the likelihood ratio (r) for various thresholds of standardized daily maximum temperature (T^*_{max}). For each threshold, values are relative to the fraction of all summer days with T^*_{max} greater than the threshold.

Region	r for T^*_{max}		
	>2.0	>1.0	>0.0
Pacific coast	1.34	1.24	1.14
Pacific inland	1.59	1.23	1.08
Southwest	1.37	1.39	1.21
Rocky Mountains	2.54	1.58	1.20
Northern Great Plains	2.47	1.69	1.26
Southern Great Plains	2.45	2.05	1.39
Gulf Coast	2.86	2.11	1.32
Southeast inland	3.35	2.35	1.39
Midwest	2.70	1.70	1.23
Northeast inland	2.63	1.57	1.20
Atlantic coast	2.21	1.57	1.21

In order to examine geographical variations in the strength of the T_{max}–W' relationship, a ''likelihood ratio'' (r) has been computed from the low-W' and all-day percentages of days with T^*_{max} above a range of thresholds at each of the 80 stations shown in Fig. 1. Specifically, for a particular threshold and station, r is defined as the ratio of the low-W' percentage (or conditional probability) to the all-day percentage (unconditional probability of observing a T^*_{max} greater than the threshold). The all-day percentage is used in lieu of a percentage derived from the normal distribution since the probabilities at the high end of the all-day PDF tend to be smaller than those at the high end of the normal distribution (Fig. 4). Values of r averaged over stations in 11 geographical regions (Fig. 1) are shown in Table 1 for $T^*_{max} > 0$, $T^*_{max} > 1$, and $T^*_{max} > 2$ standard deviations. If for a particular region and temperature threshold, the conditional and unconditional probabilities were equal, the corresponding r value would be equal to 1.0. On the other hand, when $r(T^*_{max} > 2)$, for example, reaches a value of 2, then T_{max} is twice as likely to be more than two standard deviations above normal after a low-W' day as on a randomly selected summer day. Thus, only r values that are considerably larger than one are indicative of a meaningful T_{max}–W' relationship.

Inspection of Table 1 reveals that r tends to decrease as the threshold temperature decreases. For example, at inland stations in the Southeast, r is equal to 3.35 for days with $T^*_{max} > 2$ standard deviations above normal, but only equals 1.39 for all days with above-normal T_{max}. This implies that a prolonged soil moisture deficit has a more pronounced effect on the frequency of very hot days than on the frequency of days with above-normal temperatures. Across the United States, the value of r varies considerably for high temperature thresholds but is relatively small everywhere for all days with $T^*_{max} > 0$. Overall, the inland portions of the southeastern

TABLE 2. Probability (p, in %) and likelihood ratio (r) for various thresholds of standardized daily maximum temperature (T^*_{max}) under low soil moisture conditions at humid inland, arid inland, and humid coastal stations.

	Humid inland		Arid inland		Humid coastal	
Threshold	p	r	p	r	p	r
2.0	5.1	3.3	1.2	1.6	3.7	2.4
1.0	33.9	2.3	21.7	1.4	25.2	1.8
0.0	72.6	1.4	63.8	1.2	65.7	1.3

United States exhibit the largest increase in the frequency of high daytime temperatures between normal- or high-W' conditions and low-W' conditions. Among the other inland regions, the probability of observing extremely high T_{max} is also significantly elevated during dry spells in the interior Northeast, Midwest, Great Plains, and Rocky Mountain states. Along the coasts of the Atlantic, Gulf of Mexico, and the Pacific, $r(T^*_{max} > 2)$ tends to be somewhat smaller than farther inland. However, this pattern breaks down at lower temperature thresholds. Overall, the weakest temperature–W' relationship is found along the Pacific coast, in the Pacific inland region, and in the Southwest.

These geographical differences are in general agreement with those documented by Crutcher (1978), Madden and Williams (1978), Karl and Quayle (1981), Namias (1983), Walsh et al. (1985), Karl (1986), McNab (1989), Williams (1992), Huang and van den Dool (1993), and Huang et al. (1996). However, for extreme T_{max}, the T_{max}–W' relationship is strongest in the Southeast rather than in the Southern Great Plains where precipitation–temperature and soil moisture–temperature correlations tend to be largest. It is also interesting to note that Karl and Quayle (1981) and McNab (1989) found dry summers in the Northeast to be equally likely to have above-median and below-median monthly mean temperatures, while this study shows that a relatively large fraction of daily maximum temperatures that are at least 2 standard deviations above normal occurs under low soil moisture conditions. This difference is likely to be attributable to the greater dependence of daily maximum temperatures on soil moisture as well as to the nonlinearity inherent in the soil moisture–temperature relationship.

Based on the evidence presented in Table 1, the association between T_{max} and W' appears to be strongest in inland regions that normally experience abundant rainfall and rather weak in areas that receive small amounts of rain. To further examine this relationship, PDFs of T^*_{max} under low-W' conditions and the corresponding relative likelihoods have been computed for humid inland, arid inland, and humid coastal stations (Table 2). Here, a station is considered to be located inland if it lies at least 150 km from the nearest coastline and to have a humid (dry) climate if it records more than 1000 mm (less than 300 mm) of precipitation annually. This stratification yields groups of 12 humid inland, 14 arid inland, and 8 humid coastal stations. Because, according to these definitions, only one coastal station is classified as arid, no statistics are included for the arid coastal category.

TABLE 3. Likelihood ratios (r) for $T^*_{max} > 2$ on day n after a summer low soil moisture day at humid inland, arid inland, and humid coastal stations.

n	Humid inland	Arid inland	Humid coastal
−60	1.5	0.8	1.4
−30	1.7	1.1	1.1
−15	2.0	1.4	1.4
−10	2.3	1.4	1.9
−5	2.8	1.5	2.1
−1	3.3	1.7	2.5
0	3.4	1.6	2.6
1	3.3	1.6	2.4
5	2.9	1.4	1.9
10	2.5	1.1	1.8
15	2.2	1.1	1.6
30	1.8	1.3	1.4
60	1.5	1.4	1.1

Table 2 confirms the impressions gained from Table 1. At humid inland stations, the probability of observing a $T^*_{max} > 2.0$ standard deviations is more than three times higher following the occurrence of a low-W' day than on a randomly selected day. Adjacent coastal stations exhibit a 2.4-fold increase in the same probability, while desert and semidesert locations exhibit only a 1.6-fold increase. As was apparent in Table 1, these contrasts are less pronounced for less extreme temperature thresholds.

To investigate the temporal persistence of the W'–T_{max} relationship, $r(T^*_{max} > 2)$ has also been computed for various times between 60 days prior to a low-W' day (day −60) and 60 days after a low-W' day (day +60) by shifting W' relative to the June–August T^*_{max} time series. For example, when the lag is equal to +1 day, then W' of June 1–August 30 is matched with T^*_{max} of June 2–August 31, while for a lag of +60, W' of April 3–July 2 is paired with the same set of temperatures. Table 3 shows values of $r(T^*_{max} > 2)$ as a function of the lag between W' and T^*_{max} for the same three groups of stations used to construct Table 2.

Overall, the r values are relatively symmetric about the zero lag. However, at humid inland stations, the values are slightly higher at lags between +5 and +30 days than at −5 to −30 days. At the arid inland stations, on the other hand, the r values appear to be shifted slightly toward negative lags. With increasing positive lag (i.e., following a low-W' day), $r(T^*_{max} > 2)$ decreases at approximately the same rate in each of the three regions. Since, around lag zero, the humid inland stations report the largest r values, the W'–T_{max} relationship remains significant for a greater length of time at those stations than in the other two regions. Thus, the regional differences that are very pronounced on day 1 persist to some degree for at least a month after the low-W' event. In this respect, the results of this study are con-

TABLE 4. Cross correlations × 100 of 1 Jun–31 Aug (JJA) standardized daily maximum temperatures (T^*_{max}) with T^*_{max} and soil moisture anomalies (W') for selected lags between −60 and +60 days. Correlations are computed from time series of 5-day averages and are averaged over humid inland, arid inland, and humid coastal stations. A lag of $+n(-n)$ indicates that the time series in the column heading leads (lags) the JJA T^*_{max} by n days.

	Humid inland		Arid inland		Humid coastal	
n	T^*_{max}	W'	T^*_{max}	W'	T^*_{max}	W'
−60	12	−7	6	−2	12	−5
−30	17	−13	5	−6	14	−8
−15	24	−25	8	−14	18	−17
−10	27	−33	15	−22	19	−26
−5	46	−41	35	−34	35	−37
0	100	−47	100	−36	100	−38
5	44	−29	35	−15	34	−17
10	25	−20	14	−9	18	−12
15	21	−17	8	−7	16	−11
30	15	−11	5	−4	13	−9
60	6	−10	4	−5	6	−5

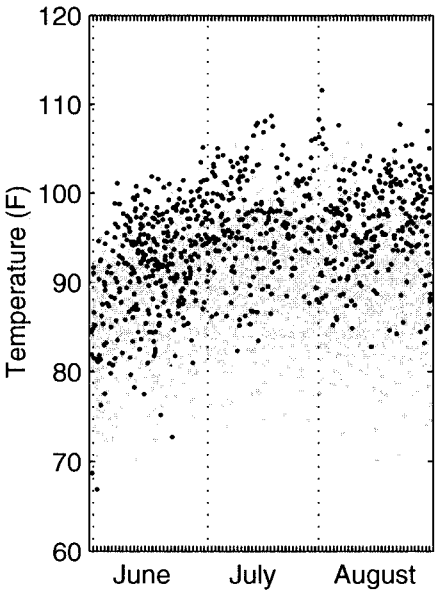

FIG. 5. As in Fig. 3, but for summer days with more than 75% of possible sunshine only.

sistent with those of previous investigations that employed monthly rather than daily data (e.g., Williams 1992; Huang and van den Dool 1993; Huang et al. 1996).

Table 4 shows the autocorrelation functions of T^*_{max} as well as cross correlations between W' and T^*_{max} for the summer season. The cross correlations are computed by shifting the time series of 5-day averages of W' backward and forward in time relative to the time series of 5-day averages of T^*_{max} for June–August. Since the autocorrelations are determined in an analogous manner, using T^*_{max} in place of W', they are not completely symmetric about the zero lag. In Table 4, the strongest soil moisture–temperature relationship is again found at humid inland stations. In contrast to the low-W' probability density functions and likelihood ratios of T^*_{max} (Tables 2 and 3), the cross-correlation functions for arid inland and humid coastal stations do not differ significantly from one another. Furthermore, the cross correlations peak at lag zero in all three regions and are considerably larger with T^*_{max} leading W' by 5 days (lag = −5) than with W' leading T^*_{max} (lag = +5). The high positive correlations at short negative lags reflect the fact that warm, dry weather tends to deplete soil moisture. Compared to the autocorrelations of T^*_{max}, the W–T^*_{max} correlations are smaller, particularly at lag +5, indicating that on a timescale of days, the persistence of T_{max} is a better predictor of T_{max} than soil moisture. However, previous work by Huang et al. (1996) suggests that a combination of W' and T_{max} should improve the T_{max} forecast, at least in humid inland regions.

5. Discussion and concluding remarks

In a prior study, Georgakakos et al. (1995) showed cross-correlation functions of 5-day averages of computed soil moisture anomalies and observed maximum temperature anomalies for the Bird Creek, Oklahoma, and the Boone River, Iowa, watersheds. For the period 1949–88, they found the correlation at Bird Creek to be as strong as −0.65 for soil moisture leading temperature by 5–10 days. In our analysis of a similar period of record, the highest negative cross correlations between T^*_{max} and W' at stations near Bird Creek tend to be somewhat smaller (−0.55) and occur at lag zero, while by lag +5, the correlations have dropped to below −0.4. The magnitude (−0.4) and lag (0) of the peak correlation in the area of Boone River, on the other hand, agree with Georgakakos et al.'s calculations. The discrepancy between our results and those of Georgakakos et al. can be attributed to the use of two substantially different models for the computation of soil moisture; in contrast to our highly simplified bucketlike one-layer model of the local water balance, Georgakakos et al. employed a more complex hydrological model with a two-layer representation of the soil that is calibrated to runoff and applied to an entire watershed. However, it is currently unclear exactly which processes are responsible for the difference in results.

Synoptic-scale circulation patterns that are favorable for strong daytime heating and a lack of precipitation may contribute to the relationship between soil moisture and T_{max}. For example, if a synoptic situation that produces a dry soil persists, there may be a tendency for the days following a low-W' day to be unusually sunny, resulting in stronger surface heating and higher daytime temperatures. Figure 5 shows the distribution of June–August daily maximum temperatures at Little Rock only on mostly sunny days, with low-W' days identified by black dots, as in Fig. 3. A day is defined as mostly sunny if the percent of possible sunshine exceeds 75%. In addition, the PDFs of summertime T^*_{max} for humid

TABLE 5. Average cumulative probability density functions of standardized daily maximum temperatures at humid inland stations for various categories of summer days (1 Jun–31 Aug). All equals all summer days, *P* equals days preceded by a day without precipitation, *W′* equals days preceded by a day with a low soil moisture anomaly, *S* equals all mostly sunny days, and *W′S* equals mostly sunny days preceded by a day with a low soil moisture anomaly.

Threshold	All	*P*	*W′*	*S*	*W′S*
2.0	1.5	2.1	5.1	1.9	7.7
1.0	14.9	19.1	33.8	18.9	44.8
0.0	53.1	61.3	72.6	62.1	82.9

TABLE 6. Average cumulative probability density functions of standardized daily maximum temperatures at humid inland stations for all Junes, Julys, and Augusts (all) as well as for the months following a May, June, or July with a low monthly precipitation anomaly (*P′*), a low end-of-the-month soil moisture anomaly (*W′*), a low *Z* index (*Z*), and a low Palmer Drought Severity Index (PDSI).

Threshold	All	*P′*	*W′*	*Z*	PDSI
2.0	1.5	3.2	3.3	3.4	3.2
1.0	14.8	23.3	24.6	24.2	23.8
0.0	52.8	61.4	62.6	62.3	62.6

inland stations on various categories of days are listed in Table 5. The clustering of black dots (low-*W′* days) toward the top of the temperature range appears to be at least as pronounced in Fig. 5 as in Fig. 3, suggesting that differences in cloudiness between low-*W′* and other days are not the primary factor accounting for the association between low *W′* and high T_{max}. The same conclusion can be drawn when comparing the clear-day and all-day PDFs for all humid stations (Table 5). Table 5 also shows that the change in the PDF of T^*_{max} is smaller following a day with no precipitation than after a low-*W′* day. This indicates that at humid inland stations, the higher percentages after a low-*W′* day are not merely a reflection of the meteorological conditions on the previous day, but also incorporate memory of prior conditions.

The strength and relatively long memory of the soil moisture–temperature relationship over the interior Southeast are consistent with the hypothesis that in this region, local evapotranspiration contributes a significant portion to summertime precipitation over the area and therefore represents an important climatic control (Brubaker et al. 1993; Eltahir and Bras 1996). Although not explicitly included in our model, transpiration from vegetation has also been identified as a significant component in the feedback between land and atmosphere (Shukla and Mintz 1982; Dirmeyer 1994; Yang et al. 1994; Koster and Suarez 1996; Xue et al. 1996). As a result of the increased sensible heat flux from a dry soil, record and near-record high temperatures are particularly likely during periods of moisture deficit over the interior Southeast. The weaker temperature–soil moisture relationship in other regions can be attributed to a persistent lack of moisture and low evapotranspiration rates in arid regions (Karl 1986) and the advection of marine air by sea breezes in coastal areas (Walsh et al. 1985).

Since the monthly Palmer *Z* index and PDSI are widely used as indicators of dry spells, it is interesting to compare the dependence of T_{max} on *W′*, the *Z* index, and the PDSI. The comparison is best made by using the end-of-the-month values of *W′*, the *Z* index, and the PDSI for May, June, and July and considering the distributions of all T^*_{max} during the month following a low value of each index, that is, a value that falls into the bottom quartile of the index's May–July values (Table 6). These distributions can be compared to the monthly distribution of T^*_{max} obtained when all Junes, Julys, and Augusts are considered, as well as to the PDF during the month following a low monthly precipitation anomaly.

The frequency of high afternoon temperatures tends to be considerably larger during a summer month after a low *P′*, *W′*, *Z* index, or PDSI than during all summer months combined. The differences among the PDFs based on *W′* and the Palmer indices are small compared to the shift in the T^*_{max} distribution between overall and dry conditions as measured by any of these three indices. Although the percentages following a low-*P′* month are consistently slightly smaller than those for low *W′*, *Z*, and PDSI months, the difference between the low-*P′* and low-*W′* PDFs is considerably less pronounced for monthly than for daily data. These results suggest that the processes that contribute to the difference between the no-precipitation and low-*W′* PDFs for daily data (Table 5) operate primarily on timescales shorter than one month. They further indicate that, in terms of capturing the summertime relationship between antecedent moisture conditions and T_{max} in humid inland regions on timescales of one month, *W′* is interchangeable with the *Z* index and the PDSI, and *P′* provides nearly as much information as any of the soil moisture indices considered in this paper.

In summary, it may be concluded from the results of this study that 1) additional information is gained when relationships between meteorological and land surface conditions are studied with daily, rather than monthly, soil moisture time series; 2) in inland regions east of the Rocky Mountains, and particularly in the Southeast, the distribution of summertime daily maximum temperatures is shifted toward higher temperatures when the soil is dry, and 3) this shift is most pronounced at the high end of the frequency distribution, that is, for near-record high temperatures. Empirical evidence of the processes responsible for the geographical variations in the strength of the soil moisture–temperature relationship may be gathered in future work by considering other variables, such as observed relative humidity and atmospheric static stability as well as computed evapotranspiration, in addition to the variables analyzed in this study.

Acknowledgments. Special thanks go to Todd P.

Mitchell for his assistance in the preparation of figures. We also thank Greg O'Donnell for his assistance in designing and assembling the water balance model used in this study. This work was supported by the National Science Foundation through the Climate Dynamics Program under Grant ATM-9805886.

REFERENCES

Alley, W. M., 1984: The Palmer drought severity index: Limitations and assumptions. *J. Climate Appl. Meteor.*, **23,** 1100–1109.

Batjes, N. H., 1996: Development of a world data set of soil water retention properties using pedotransfer rules. *Geoderma*, **71,** 31–52.

Bravar, L., and M. L. Kavvas, 1991: On the physics of drought. I. A conceptual framework. *J. Hydrol.*, **129,** 281–297.

Bristow, K. L., and G. S. Campbell, 1984: On the relationship between incoming solar radiation and daily maximum and minimum temperature. *Agric. For. Meteor.*, **31,** 159–166.

Brubaker, K. L., D. Entekhabi, and P. S. Eagleson, 1993: Estimation of continental precipitation recycling. *J. Climate*, **6,** 1077–1089.

Buffo, J., L. Fritschen, and J. Murphy, 1972: Direct solar radiation on various slopes from 0° to 60° North latitude. USDA Forest Service Research Paper PNW-142. [Available from National Forest Service, P.O. Box 96090, 14th and Independence Avenue, SW, Washington, DC 20090-6090.]

Chang, F.-C., and J. M. Wallace, 1987: Meteorological conditions during heat waves and droughts in the United States Great Plains. *Mon. Wea. Rev.*, **115,** 1253–1269.

Crutcher, H. L., 1978: Temperature and precipitation correlations within the United States. NOAA Tech. Rep. EDS 26, NTIS Rep. NOAATREDS26; NOAA78022101, 42 pp.

Diaz, H. F., 1983: Drought in the United States—Some aspects of major dry and wet periods in the contiguous United States, 1895–1981. *J. Climate Appl. Meteor.*, **22,** 3–16.

Dirmeyer, P. A., 1994: Vegetation stress as a feedback mechanism in midlatitude drought. *J. Climate*, **7,** 1463–1483.

Eltahir, E. A. B., and R. L. Bras, 1996: Precipitation recycling. *Rev. Geophys.*, **34,** 367–378.

Georgakakos, K. P., D.-H. Bae, and D. B. Cayan, 1995: Hydroclimatology of continental watersheds. 1. Temporal analysis. *Water Resour. Res.*, **31,** 655–675.

Hollinger, S. E., and S. A. Isard, 1994: A soil moisture climatology of Illinois. *J. Climate*, **7,** 822–833.

Huang, J., and H. M. van den Dool, 1993: Monthly precipitation–temperature relations and temperature prediction over the United States. *J. Climate*, **6,** 1111–1132.

——, ——, and K. P. Georgakakos, 1996: Analysis of model-calculated soil moisture over the United States (1931–1993) and applications to long-range temperature forecasts. *J. Climate*, **9,** 1350–1362.

Karl, T. R., 1986: Relationships between some moisture parameters and subsequent seasonal and monthly mean temperature in the United States. Programme on Long-Range Forecasting Research Report Series, No. 6, WMO/TDD-No. 87, 2, 661–670. [Available form WMO, Office for Information and Public Affairs, 41, avenue Giuseppe-Motta, 1211 Geneva 2 / Switzerland; E-mail: PubSales@gateway.wmo.ch.]

——, and R. G. Quayle, 1981: The 1980 heat wave and drought in historical perspective. *Mon. Wea. Rev.*, **109,** 2055–2077.

Kimball, J. S., S. W. Running, and R. Nemani, 1997: An improved method for estimating surface humidity from daily minimum temperature. *Agric. For. Meteor.*, **85,** 87–98.

Koster, R. D., and M. J. Suarez, 1996: The influence of land surface moisture retention on precipitation statistics. *J. Climate*, **9,** 2551–2567.

Madden, R. A., and J. Williams, 1978: The correlation between temperature and precipitation in the United States and Europe. *Mon. Wea. Rev.*, **106,** 142–147.

Manabe, S., J. Smagorinsky, and R. F. Strickler, 1965: Simulated climatology of a general circulation model with a hydrologic cycle. *Mon. Wea. Rev.*, **93,** 769–798.

McNab, A. L., 1989: Climate and drought. *Eos, Trans. Amer. Geophys. Union*, **70, 873,** and **882–883**.

Namias, J., 1960: Factors in the initiation, perpetuation and termination of drought. Extract of Publ. 51, International Association of Hydrological Sciences (IAHS) Commission of Surface Waters, 81–94. [Available from IAHS Press, Institute of Hydrology, Wallingford, Oxfordshire OXl0 8BB, United Kingdom.]

——, 1983: Some causes of United States drought. *J. Climate Appl. Meteor.*, **22,** 30–39.

National Climatic Data Center, cited 1998a: Summary of the day—first order: TD-3210 online data format documentation. [Available online from ftp.ncdc.noaa.gov.]

——, cited 1998b: Time bias corrected divisional temperature–precipitation–drought index: TD-9640 tape documentation. [Available online from ftp.ncdc.noaa.gov.]

Palmer, W. M., 1965: Meteorological drought. Research Paper 45, U.S. Weather Bureau, 58 pp. [Available from NOAA Library and Information Services Division, Washington, DC 20852.]

Priestley, C. H. B., and R. J. Taylor, 1972: On the assessment of surface heat flux and evaporation using large-scale parameters. *Mon. Wea. Rev.*, **100,** 81–92.

Rind, D., 1982: The influence of ground moisture conditions in North America on summer climate as modeled in the GISS GCM. *Mon. Wea. Rev.*, **110,** 1488–1494.

Shukla, H., and Y. Mintz, 1982: The influence of land surface evapotranspiration on the earth's climate. *Science*, **215,** 1498–1501.

Stamm, J. F., E. F. Wood, and D. P. Lettenmaier, 1994: Sensitivity of a GCM simulation of global climate to the representation of land-surface hydrology. *J. Climate*, **7,** 1218–1239.

Swift, L. W., Jr., 1976: Algorithm for solar radiation on mountain slopes. *Water Resour. Res.*, **12,** 108–112.

Walsh, J. E., W. H. Jasperson, and B. Ross, 1985: Influence of snow cover and soil moisture on monthly air temperatures. *Mon. Wea. Rev.*, **113,** 756–768.

Williams, K. R. S., 1992: Correlations between Palmer drought indices and various measures of air temperature in the climatic zones of the United States. *Phys. Geogr.*, **13,** 349–367.

Xue, Y., M. J. Fennessy, and P. J. Sellers, 1996: The impact of vegetation properties on U.S. summer weather prediction. *J. Geophys. Res.*, **101,** 7419–7430.

Yang, R., M. J. Fennessy, and J. Shukla, 1994: The influence of initial soil wetness on medium-range surface weather forecasts. *Mon. Wea. Rev.*, **122,** 471–483.

Yeh, T. C., R. T. Wetherald, and S. Manabe, 1984: The effect of soil moisture on the short-term climate and hydrology change—A numerical experiment. *Mon. Wea. Rev.*, **112,** 474–490.

Zhao, W., and M. A. Khalil, 1993: The relationship between precipitation and temperature over the contiguous United States. *J. Climate*, **6,** 1232–1236.